https://doi.org/10.52131/jmps.2020.0102.0006

Journal of Materials and Physical Sciences

Volume 1, Number 2, 2020, Pages 48 - 57

Journal Homepage:
https://journals.internationalrasd.org/index.php/jmps

JOURNAL OF MATERIALS AND PHYSICAL SCIENCES
INTERNATIONAL RESEARCH ASSOCIATION FOR SUSTAINABLE DEVELOPMENT

Synthesis and Characterization of Rare Earth (Ce) Substituted Magnesium Ferrite $MgCe_{0.1}Fe_{1.9}O_4$ and Banana Peel $BPMgCe_{0.1}Fe_{1.9}O_4$

Atiq ur Rehman[1], Mukhtar Ahmad[2*]

[1] Department of Physics, Riphah international university, Lahore
[2] Department of Physics, COMSATS University Islamabad, Lahore Campus, Lahore

ARTICLE INFO

Article History:
Received: August 13, 2020
Revised: October 28, 2020
Accepted: November 18, 2020
Available Online: December 31, 2020

Keywords:
Hydrothermal method
Fourier transform infrared
Spinel ferrites
FCC structure
Soft ferrites

ABSTRACT

In this study, a composite of cerium doped magnesium ferrite ($MgCe_xFe_{2-x}O_4$, x= 0.1) and banana peel powder was prepared by hydrothermal method. Crystal structure and phase identification, chemical bonding, and magnetic properties were characterized by X-ray diffraction (XRD), Fourier transform infrared (FTIR) and vibrating sample magnetometry (VSM), respectively. XRD results reveal that the prepared ferrite exhibits single phase face centered cubic (FCC) structure having no impurity in the sample. Addition of banana peel powder has no effect on the crystal structure. The values of structural parameters greatly match with the earlier reported values for the same structure. FTIR results clearly indicate that the prepared ferrite is spinel and have well defined vibrational and stretching peaks due to different molecules present in the compound. Coercivity values for both ferrite and composite materials are found to be a few hundred Oersted which confirm the soft magnetic nature of this ferrite. The observed parameters show that the prepared composite may find technological application for microwave absorption and multi-layer chip inductors.

*Corresponding Author's Email: ahmadmr25@yahoo.com

1. Introduction

Nano sized spinel ferrites possess interesting electrical and magnetic features for various technological applications including high frequency devices, supercapacitors, photocatalytic and wastewater treatment (Greenwood & Earnshaw, 2012). The hydrothermal method will be used to prepare rare earth Ce-substituted ($MgCe_xFe_{2-x}O_4$, x= 0.1) monoferrite with enhanced magnetization and higher active functional sites for easy magnetic separation. Substitution of Ce may affect DC resistivity, AC conductivity and magnetic properties and the substituted material can be used at higher working frequencies where low eddy current losses are desirable. In addition, Ce ions can be used to improve the remanence magnetization and decrease the dielectric loss, respectively but these ions cause reduction in the saturation magnetization, coercivity and permeability of the material and thus cannot be used for microwave devices. Ferrites substituted with rare earth (Ce) may alter the number of active sites through magnetic, electrical and physical properties can be enhanced (Datta, Deb, & Tyagi, 1996; Gaumat, Rastogi, & Misra, 1992; Pickering, 1985). The doping with rare earth at both Mg and Fe site is good choice. The dissimilar ionic radius of (Ce) compared to Fe will introduce structural distortions, thus modifying the Fe-O, Mg-O bond lengths and Fe-O-Fe bond angles. (high cost) This modification will lead to the optimum magnetic and dielectric properties of the material. Moreover, the charge compensation due to different valance states of Fe compared to Ce will create vacancies of oxygen and the fluctuation of the iron valency due to different valence states which will effectively improve the electrical properties. Thus, increased electrical resistivity causes to

reduce eddy currents which are beneficial for a material working at higher frequencies. Hence, it is worth studying the structural, elastic and magnetic properties of rare earth-substituted $MgCe_{0.1}Fe_{1.9}O_4$ and Banana Peel $BPMgCe_{0.1}Fe_{1.9}O_4$. Different methods are used to difluoride water such as electrolysis, reverse permeation, ion exchange, chemical precipitation and adsorption (Goraya, 2021).

The method of removing fluoride depends on factors such as capital and operational cost. operating cost, environmental impact and fluorine removal efficiency method. For example, distillation has the ability to remove ions from water, but it is very expensive. This electro dialysis method uses ion exchange membranes and electric potential removal of different types of ions from aqueous solutions (Rehman, Yusoff, & Alias, 2015). It has a cation and anion exchange membranes between cathode and anode. The cations migrate when they fall negative ions increase. These ions penetrate the membrane and are retained through oppositely charged electrodes (Wang et al., 2013). The limitation of this method has low efficiency of trace removal concentrations of pollutants in aquatic media (Chen et al., 2016).

Ion exchange process can also be used in which ions removed from an aqueous solution and are replaced by another type of ion. Ion exchange confirms the passage of water by exchanging polymer ions, it is a water-insoluble substance that can exchange some of its ions with similarly charged ions in an aqueous media. Many natural organic materials contain ions exchange properties or it can be added to them by chemical modification. This function has been used to produce ionic spare parts from natural materials. Use nitric acid as an oxidant to modify wood, fiber, peat and carbon concentrated sulfuric acid is used to introduce sulfonic acid groups. Muhammad Abdur Rehman. et al. (2015) prepared a series of doped and un-doped magnetic ferrites $CuCe_xFe_{2-x}O_4$ (x=0.0---0.5) Doped ferrite proved superior with respect to functional growth sites and adsorption of fluoride. Fluoride adsorption capacity was adversely affected by the presence of associated anions such as HCO_3^{-1}, $SO4^{-2}$, $NO3^{-1}$, $Cl^{-1}$and As. These anions compete for ferrite active sites during adsorption (Rehman et al., 2015). Jing Wang at el. (2013) Prepared C_e-Z_rO_2 nanocages for fluoride removal from water and investigated their performance. The prepared adsorbent showed good adsorption capacity in 3-7 pH range. The optimal pH range was 3.4--4.5. At pH 4.0 the capacity was found to be as high as 175mg/g. Simultaneous presence of chloride and arsenate in high concentration reduced fluoride adsorption. Presence of sulphate had no effect but HCO_3^- reduced efficiency. Electrostatic interaction and anion exchange were reported to pay key role in fluoride removal mechanism (Wang et al., 2013).

Magnetic ferrite ($MgFe_2O_4$) is efficient for various applications of ferrites. Doping with cerium (Ce) enhances adsorption capacity of $MgCe_xFe_{2-x}O_4$ by increasing active functional sites and dispersion of particles. Addition of banana peels powder further improves the adsorption ability of $MgCe_xFe_{2-x}O_4$. Therefore, we have a plan to investigate the $MgCe_xFe_{2-x}O_4$/Banana peels composite ions different applications.

2. Synthesis Techniques

2.1. Synthesis of Magnetic Ferrite by Hydrothermal Method

33.3ml aqueous solution of metal chlorides with concentration 1mol/L was prepared for each $MgCl_2$, $CeCl_3.8H_2O$ and $FeCl_3.6H_2O$. It was achieved by dissolving 3.7g of $MgCl_2$, 1.3g of $CeCl_3.8H_2O$ and 17.12g of $FeCl_3.6H_2O$ in 33.3ml deionized water in separate beakers. Each beaker, except for that containing $FeCl_3.6H_2O$ was covered with aluminum lid. Each container was placed on hot magnetic plat (at 60 °C) for 30 minutes while stirring the solution during this interval. Then the contents of all three containers were mixed. The sample so obtained was stirred for 2 hours on hot magnetic plate at 60 ℃. Then the contents were left to cool to room temperature and then were transferred in Teflon lined stainless steel autoclave. The autoclave with its contents was placed in a gradually heated oven (at 180 ℃) for 6 hours. Then the oven was put off to cool the contents to room temperature. The sample was washed thrice by deionized water to eliminate chlorides. After that the contents were placed in a gradually heated dry oven at (60 ℃) for 24 hours. The final product was our required ferrite in powder form.

Flow chart below depicts the procedure for synthesizing magnesium ferrite is shown in Figure 1.

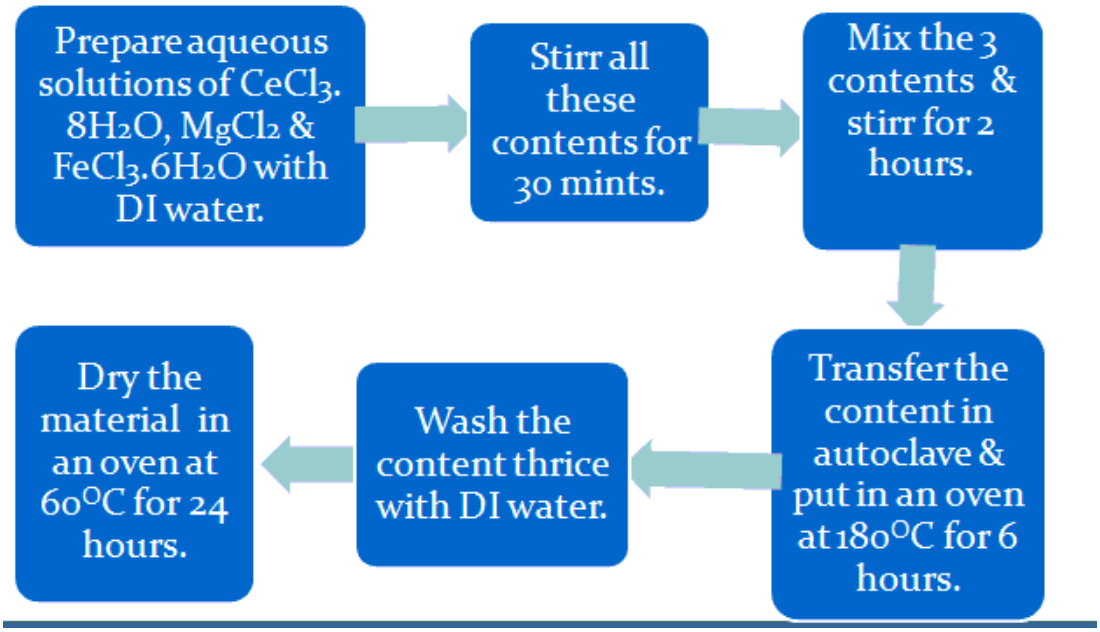

Figure 1: Flow chart of preparation procedure of magnesium ferrite

2.2. Preparation of Banana Peel Dust

Banana peels were collected and washed thoroughly, first with tap water and then with deionized water. Then these peels were placed in a dry oven at 60°C for 12 hours. After that the peels were broken into small pieces and again were left for 24 hours in the oven at 60°C. Finally, the dried peels were crushed in kitchen grinder. Following flow chart summarizes the procedure for preparing banana peel powder.

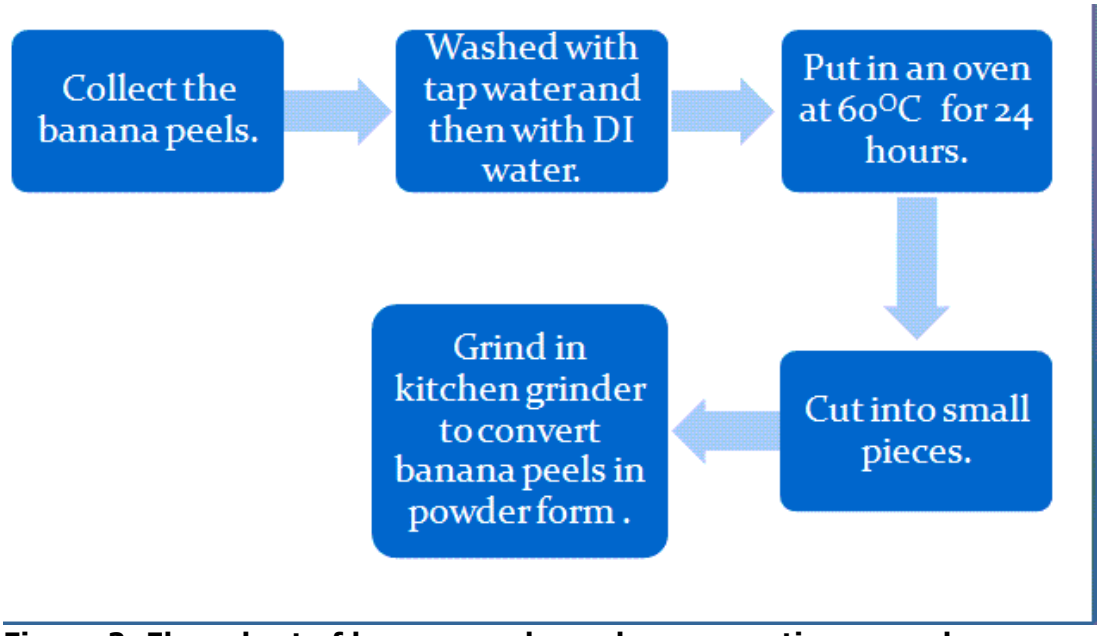

Figure 2: Flow chart of banana peel powder preparation procedure

3. Results and Discussion

3.1. X-Ray Diffraction (XRD) Analysis

XRD technique was applied to synthesized magnesium ferrite. Sample material was heated at 180 ℃ for 12 hours. Match software was used for phase identification and analyzing average crystalline size, crystal structure and lattice parameters. The index patterns (Figure 3) matched with JCPDS card number 00-017-0464 (ICDD -01-073-1720).

This indicates that crystals are face centered cubic in structure having space group Fd3m and space group number is 227. Average crystalline size was determined using Scherer's equation.

$$D=K\,\lambda/\beta\,\cos\theta \qquad (1)$$

D being crystallite size, λ is wavelength of radiations emitted by copper source, β the full width at half maximum and θ the angle of diffraction. The value was found to be 15.76 nm for ($MgCe_xFe_{2-x}O_4$) ferrite.

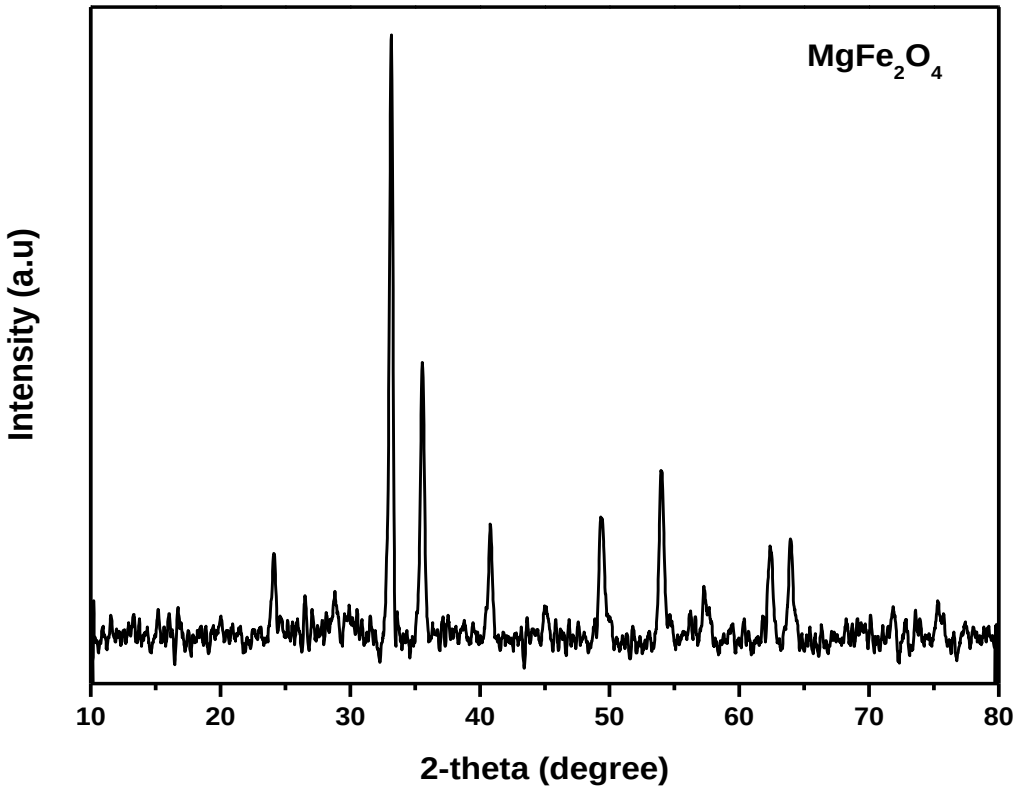

Figure 3: XRD graph for magnesium ferrite

Table 1
Lattice parameters for magnesium ferrite

Hkl	2θ (degrees)	θ (degrees)	a (Å)
220	33	16.5	6.1
311	36	18	8.2
400	42	21	8.597
422	49	24.5	9.09
511	54	27	8.81
440	62	31	8.41
442	68	34	8.26
533	75	37.5	2.52

Average value of a = 7.498 (Å), Volume (a^3) = 421.5379 $Å^3$, X-ray density ($D_x = 8M/N_AV$) = 6.3 g/cm^3

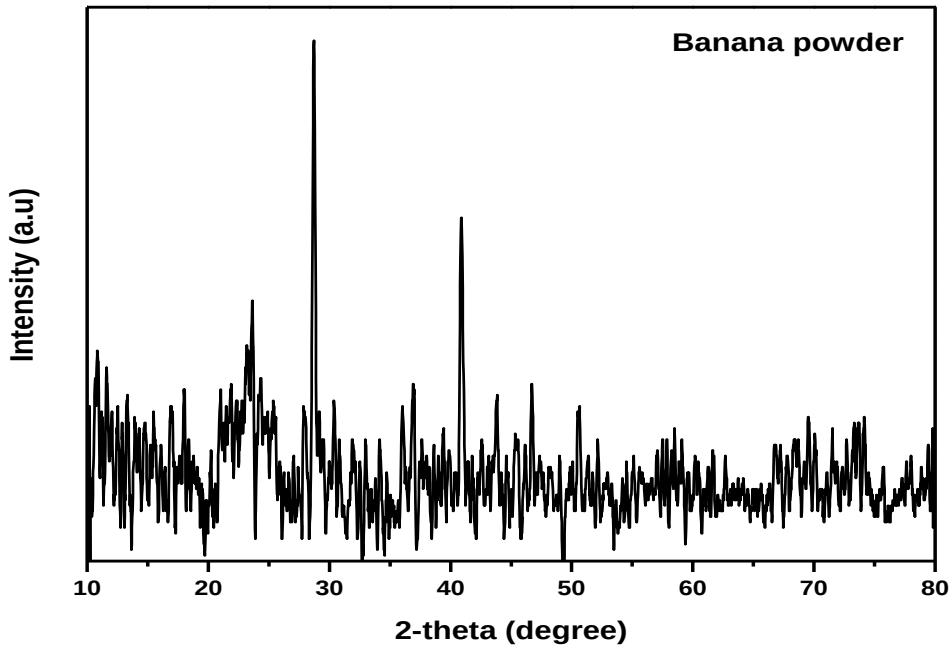

Figure 4: Graph of XRD result for banana peel powder

Banana peel is amorphous material. It contains minerals, nutrients and fabrics. Concentration of minerals is as under table 2.

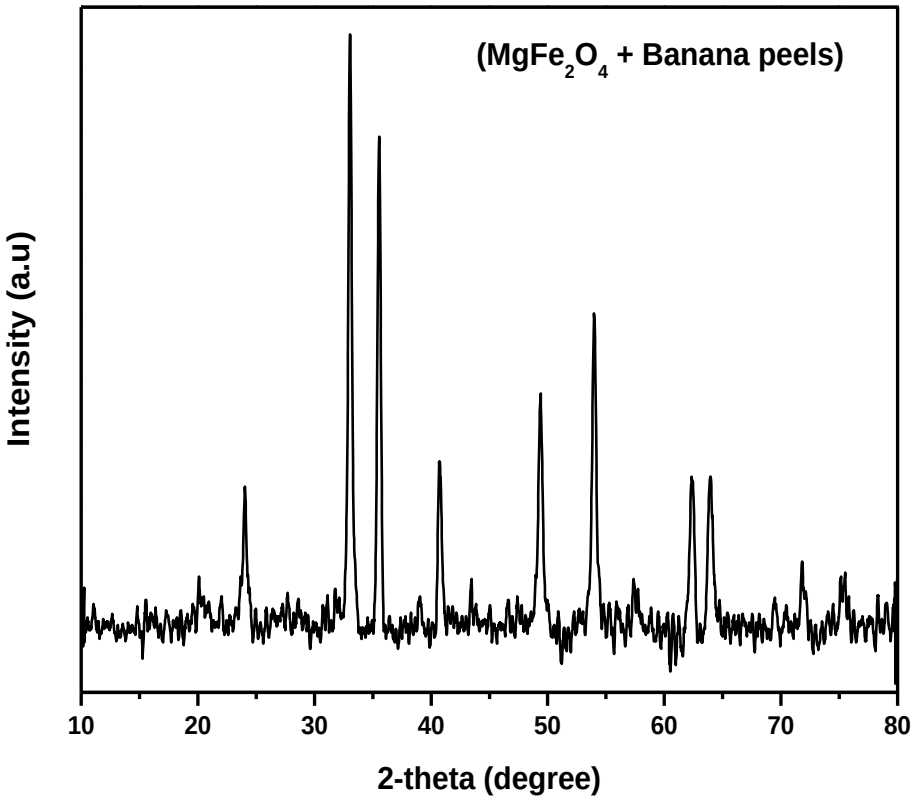

Figure 5: Graph of XRD result for composite material

Table 2
The concertation table of Minerals

Minerals	Concentration (mg/g)
K	78.10
Mn	76.20
Na	29.30
Ca	19.20
Fe	0.61

Table 3
Lattice parameters for composite material

Hkl	2θ (degrees)	θ (degrees)	a (Å)
200	20	10	8.2
221	24	12	10.4
331	33	16.5	11.8
522	36	18	6.89
400	38	19	9.46
422	48	24	9.27
611	54	27	10.4
440	64	32	8.22
620	72	36	8.28
534	75	37.5	8.9

Cell volume = 580.09 ($Å^3$), X-ray density = 2.8g/cm^3, Crystalline size =17.8nm

3.2. Fourier Transform Infrared Spectroscopy (FTIR)

Graph of FTIR for the prepared composite shows absorption band at around 535cm^{-1}. These bands are the results of stretching vibrations of Fe^{3+}–O_2 on tetrahedral and octahedral sites suggesting magnesium ferrites to be inverse spinel. Symmetric vibration of NO_3 group caused band at 1384cm^{-1}. Bands at 3410 and 2922 cm^{-1} can be attributed to stretching O–H vibrations. Absorption band at 1625 cm^{-1} is caused by the bending of water molecules. Bands at 3573cm^{-1} and 632 cm^{-1} are distinguishing features of O–H stretching vibrations. At 3423 and 1639 cm^{-1}stretching and bending of adsorbed molecules of water can be noted. The band occurring at 3446 cm^{-1} and those existing at 1638cm^{-1} and 1121 cm^{-1} are due to the symmetric stretching vibrations of O–H groups and hydrogen-bonded surface molecules respectively. This suggests the presence of absorbed or free water in the sample. From these vibrations it is concluded that the sample still retains hydroxyl groups. Band at 1380 cm^{-1} is the characteristics of symmetric vibration of NO_3^- group. Sharp band at 997 cm^{-1} is the indication of Mg-based ferrite. Vibrations of metal oxide are generally below 1000cm^1. So, the peaks at 997 and 710 cm^{-1} show the presence of Fe-O bonding. Existence of band around 475 cm^{-1} confirms the spinal structure of prepared material.

On the spectrum obtained for pure magnesium ferrite, broad peeks occur at 592cm^{-1} and 631 cm^{-1}. These peaks occur due to Fe–O bond stretching vibrations which indicate that tetrahedral sites are occupied by Feþ3 ions. Splitting of n1 band at 570 cm^{-1}, is associated with Fe–O bond of Fe_3O_4. A weak peak is formed at 434 cm^{-1}which appears due to the presence of Feþ3 –O_2 bond at octahedral sites. Existence of these peaks indicate spinel structure of Fe_3O_4. Existence of broad peak at 3446cm^{-1} and sharp peak at 1635 cm^{-1} is caused by stretching and bending of vibrations of hydroxyl group. Occurrence of these peaks is clear indication of adsorption of water at the surface of Fe_3O_4. Peaks formed at 1242 cm^{-1}, 1193 cm^{-1} and 1149 cm^{-1} occurred due to symmetrical stretching vibrations and ester bond. A broad band at 3442 cm^{-1} is attributed to hydroxyl stretching vibrations. Peak at 590 cm^{-1} shows presence of ferric oxide particles. The peaks at 3446 cm^{-1} and 1635 cm^{-1} are the evidence of the existence of adsorbed water. 550 cm^{-1} band is the identification of cubic crystalline forms of cerium which shows that cerium ions occupy octahedral sites. Interplanar distance increases when Feþ2 ions are replaced by Ceþ4 ions. The peak at 726 cm^{-1} is generated by the vibrations of Ce–O ions. The spinel structure of the filler material is confirmed by these results.

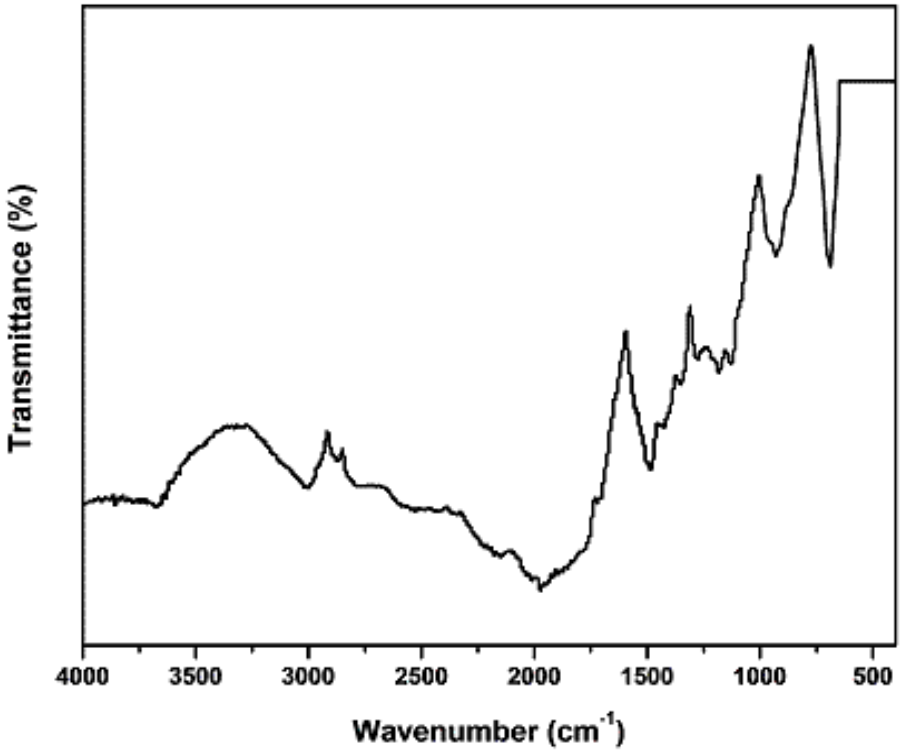

Figure 6: FTIR graph for composite material

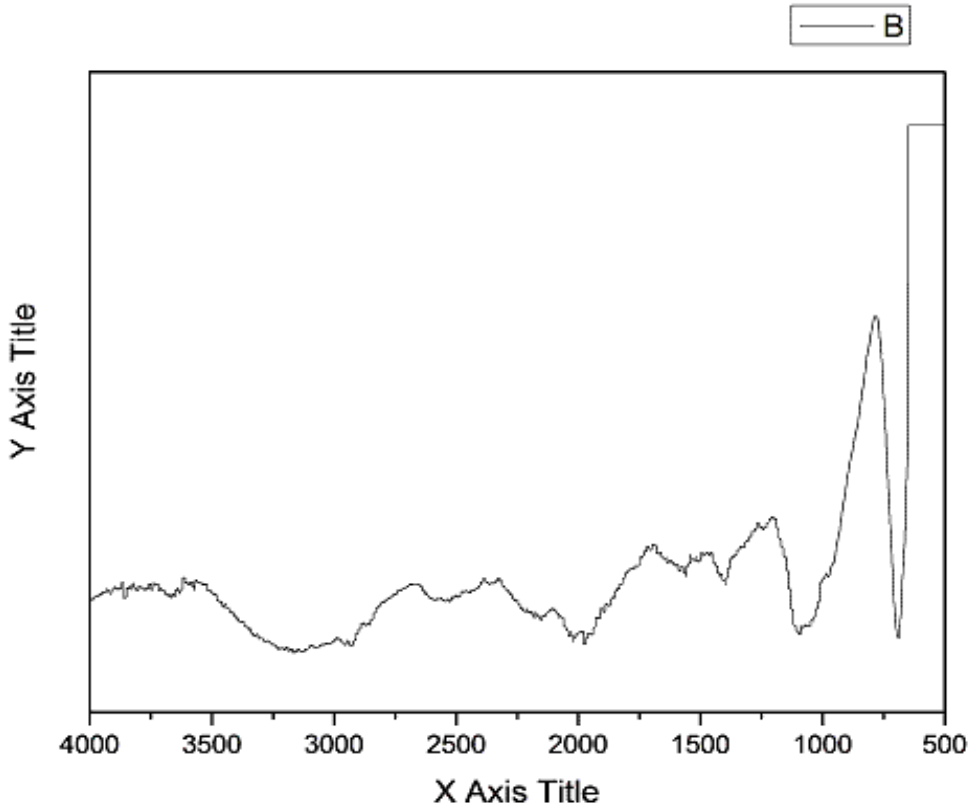

Figure 7: FTIR graph for banana powder

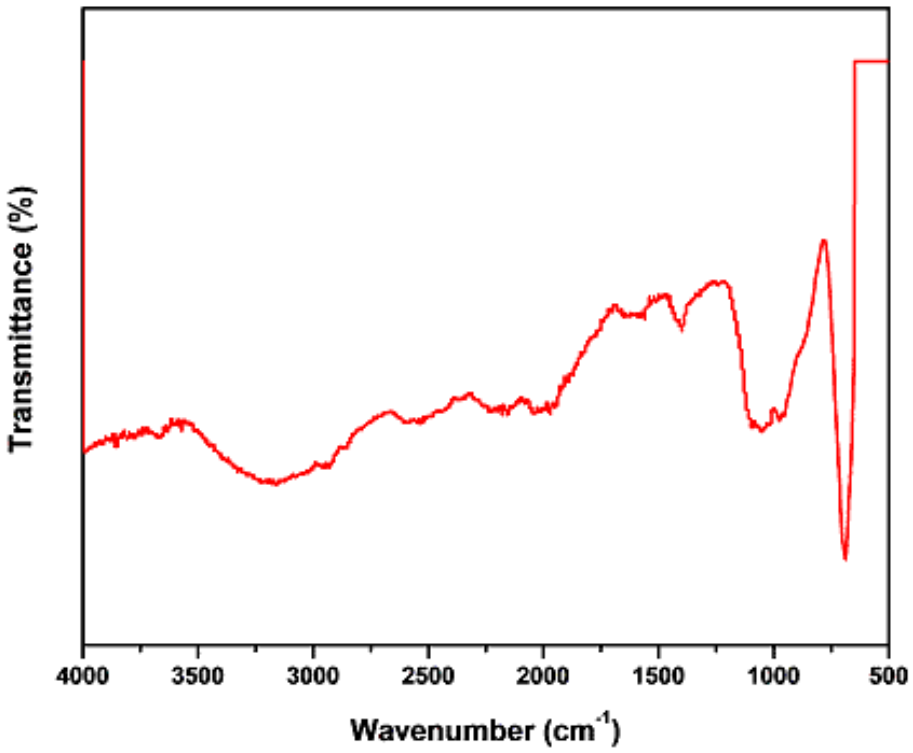

Figure 8: FTIR graph for magnesium ferrite

3.3. Vibrating Sample Magnetometer (VSM)

Magnetic measurements were carried out by vibrating sample magnetometer. The magnetic properties of synthesized pure magnesium ferrite and its composite with banana peel powder were determined at room temperature for applied field range from -8000 to +8000 Oe as shown in figure 9. The Stoner-Wolfforth model was used to calculate the magnetic saturation, the relation is as under:

$$M(H) = Ms\,(1-H_a^2 \sin\theta / 8H^2) \qquad (2)$$

Where Ms = magnetic saturation, H_a = anisotropy field, θ = angle b/w M and H. The Ms value obtained from M-H loop for pure ferrite was 47emu/g and for composite with banana peel powder was 42emu/g. The magnetic moment (n_B) was calculated by using the formula:

$$n_B\,(\mu_B) = M \times Ms/5585 \qquad (3)$$

Here M is the molecular weight of the sample and Ms is the saturation magnetization. Magnetic moment of magnesium ferrite is found to be 1.78 and that for composite material is 1.550. The remnant magnetization (Mr) is the magnetization left behind after removing applied field. The value of remnant magnetization was determined from hysteresis loop. Mr value for magnesium ferrite was 8 emu/g and for its composite with banana peel powder is 7.2 emu/g. Coercivity is the strength of the field in reverse direction which reduces sample magnetization to zero. The coercivity of pure magnesium ferrite is 155 Oe and that of composite material is 150 Oe. The squareness, that is, the ratio Mr and Ms is an importantant application of ferromagnetic material. This value for magnesium ferrite and its composite with banana peel powder is 0.16 and 0.19 respectively. Magnetic anisotropy K was calculated using the relation:

$$Hc = 0.96 \times K / Ms \quad (4)$$

Table 4
Magnetic properties of $MgFe_2O_4$ and $MgFe_2O_4$ + Banana peel powder

Property	$MgFe_2O_4$	$MgFe_2O_4$+ Banana peel powder
Ms(emu/g)	48 emu/g	42 emu/g
Mr(emu/g)	8emu/g	7.2emu/g
Mr/Ms	0.16	0.20
$u_B(n_B)$	1.718	1.50
K (magnetic anisotropy)	7750	6562.5
Hc (Oe)	155Oe	150Oe

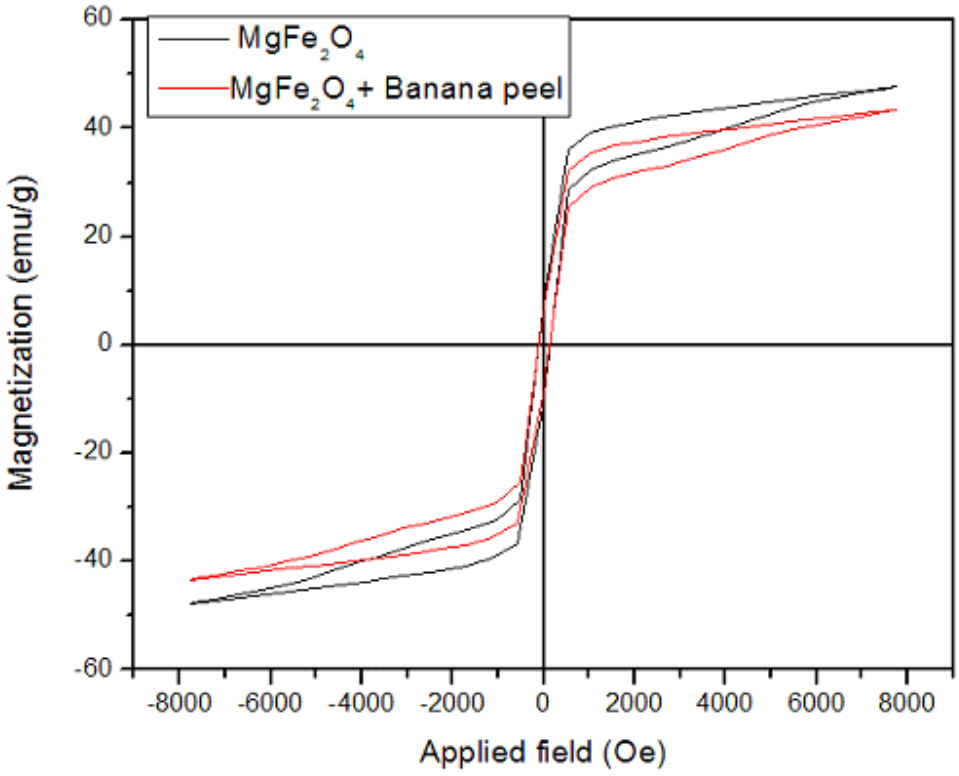

Figure 9: Magnetization variation at room temperature with applied magnetic field for $MgFe_2O_4$ and its composite with banana peel powder

Value of K for $MgFe_2O_4$ and prepared sample of the composite is found to be 7750 and 6562.5, respectively. Thin hysteresis loop indicates low coercivity and retentivity of the sample and suggests that the material is soft ferrite. Banana peel is non-magnetic in nature; hence its addition to magnesium ferrite reduced Ms values of the composite. Coercivity (Hc) of the magnesium ferrite is slightly higher than that for the composite. It is because of the large particle size of magnesium ferrite due to addition of peels. In order to obtain better soft behavior banana peel powder is added which results in lowering magnetic saturation and coercivity. The hysteresis loop for the composite material is thinner as compared to that for pure magnesium ferrite. The obtained magnetic parameters may be suitable for adsorption of fluoride from water body.

4. Conclusion

In this work, cerium doped magnesium ferrite and its composite of with banana peel were successfully synthesized using hydrothermal method. XRD results revealed the crystal structure of magnesium ferrite to be face centered cubic having volume 587.43Å^3 and X-ray density 6.3g/cm^3. The crystal structure for the composite remains unaltered because of the amorphous nature of banana peels powder. Crystallite size for $MgFe_2O_4$ was determined as 15.76 nm. FTIR clearly shows that sample material is spinel ferrite having well defined stretching and bending vibration modes. Values of Ms,n_B, Mr, Hc, Mr/Ms and K for pure

$MgFe_2O_4$ are 48emu/g, 1.718, 8emu/g, 155Oe, 0.16 and 7750, respectively. These values for the fabricated composite material in the same order are 42emu/g, 1.50, 8emu/g, 150Oe, 0.19 and 6562.5, respectively. These results and the shape of hysteresis loops clearly indicate that prepared material is soft ferrite. FTIR clearly shows that sample material is spinel ferrite having well defined stretching and bending vibration modes. The observed parameters of the materials suggest that they may find applications in different fields such as transformer cores, multilayer chip inductors (MLCIs) and most importantly in treating the fluoride contaminated water body.

References

Chen, L., Zhang, K.-S., He, J.-Y., Xu, W.-H., Huang, X.-J., & Liu, J.-H. (2016). Enhanced fluoride removal from water by sulfate-doped hydroxyapatite hierarchical hollow microspheres. *Chemical Engineering Journal, 285*, 616-624. doi:https://doi.org/10.1016/j.cej.2015.10.036

Datta, P. S., Deb, D. L., & Tyagi, S. K. (1996). Stable isotope (18O) investigations on the processes controlling fluoride contamination of groundwater. *Journal of Contaminant Hydrology, 24*(1), 85-96. doi:https://doi.org/10.1016/0169-7722(96)00004-6

Gaumat, M., Rastogi, R., & Misra, M. (1992). Fluoride level in shallow groundwater in central part of Uttar Pradesh. *Bhu-Jal News, 7*(2), 17-19.

Goraya, N. R. (2021). *Synthesis of Magnesium Ferrite (MgCexFe2-xO4)/Banana Peel Composite for De-Fluoridation of Real Water Body.*

Greenwood, N. N., & Earnshaw, A. (2012). *Chemistry of the Elements*: Elsevier.

Pickering, W. (1985). The mobility of soluble fluoride in soils. *Environmental Pollution Series B, Chemical and Physical, 9*(4), 281-308. doi:10.1016/0143-148X(85)90004-7

Rehman, M. A., Yusoff, I., & Alias, Y. (2015). Fluoride adsorption by doped and un-doped magnetic ferrites CuCexFe2-xO4: Preparation, characterization, optimization and modeling for effectual remediation technologies. *Journal of Hazardous Materials, 299*, 316-324. doi:https://doi.org/10.1016/j.jhazmat.2015.06.030

Wang, J., Xu, W., Chen, L., Jia, Y., Wang, L., Huang, X.-J., & Liu, J. (2013). Excellent fluoride removal performance by CeO2–ZrO2 nanocages in water environment. *Chemical Engineering Journal, 231*, 198-205. doi:https://doi.org/10.1016/j.cej.2013.07.022